2014 International Joint Conference on Neural Networks (IJCNN)
July 6-11, 2014, Beijing, China

Sideslip angle soft-sensor based on neural network left inversion for multi-wheel independently driven electric vehicles

Penghu Miao, Guohai Liu, Duo Zhang, Yan Jiang, Hao Zhang and Huawei Zhou

***Abstract*—Effective estimation of vehicle states such as the yaw rate and the sideslip angle is important for vehicle stability control. Unfortunately the devices are very expensive to measure the sideslip angle directly and are not suitable for ordinary vehicle. Therefore, it must be estimated. A novel sideslip angle soft-sensor using neural network left inversion (NNLI) is presented for the in-wheel motor driven electric vehicle (EV). The innovation of the presented algorithm is not only little concerned with reference model parameters identification, but also uses the characteristic of the in-wheel motor driven EV. Longitudinal acceleration, lateral acceleration, yaw rate, longitudinal velocity, steering angle, the torque of in-wheel motor which can be acquired by ordinary sensors are used as inputs. Co-simulations are carried out to demonstrate the effectiveness of the proposed soft-sensor with Simulink and CarSim.**

I. Introduction

DUE to energy conservation and environmental protection, electric vehicles (EVs) have been popular in both academic and industry. Compared with the conventional vehicles, EVs with in-wheel motors have several advantages in motion control [1]-[3]. The torque generated by in-wheel motor is accurate and fast. The driving torque of each wheel can be easily measured from the motor current and can be controlled independently.

Nowadays vehicle stability control systems have been introduced to handle the problem that it's difficult to drive a vehicle at low adhesion well. Such as the direct yaw-moment control (DYC) can be easier to realize because of the unique power trains of EVs, epically for multi-wheel independently driven EVs. In DYC system, it is required to accurately measure the yaw rate and the sideslip angle. Unfortunately, the direct measurement of the sideslip angle is only provided by special devices such as optical sensors or global positioning system (GPS) inertial sensors, which are very expensive and however unsuitable for the ordinary vehicles. Thus the sideslip angle must be estimated in real-time.

Many kinds of estimation methods have been used to estimate the sideslip angle. Based on the linear vehicle model a state observer with kalman filter is designed to estimate the sideslip angle [4], [5]. But these methods are not robust against the parameters changes in tire-road friction and driving conditions. To deal with the above problem, a fuzzy observer was proposed with non-linear vehicle model in [6]. In [7], extended and unscented kalman filters were presented to deal with its non-linearity. Based on the tire-road friction adaptation, an adaptive sideslip angle observer was presented in [8-9]. A novel method which combined the vehicle-model-based method and the kinematics-based method was proposed in [10]. In recent years, several researchers have presented the estimation using GPS without knowing the vehicle model [11].

To estimate the sideslip angle, some attempts of applying the neural network (NN) technique can be found in [12-14]. But the complex layout of the estimator generated a high computational effort. In [13], the function of the yaw rate and the lateral acceleration at instants was used to estimate the sideslip angle at the instant, but it's unsuitable when changes happened in vehicle speed and tire-road friction coefficient. In [14] the NN-based observer with the non-linear vehicle model was obtained, but it was not ideal when the vehicle speed was changed. Furthermore, these NN-based methods were seldom theoretically proved for the parameters selection during the training.

Given the above considerations, this paper will theoretically validate the input parameters selection of NN left inversion (NNLI). In the meantime, the presented soft-sensor considers the characteristics of EVs and imports the torque of motor as the input of the NNLI. This paper is organized as follows. Section II introduces the non-linear model of the multi-wheel independently driven EV. Sections III describes briefly the theory of NNLI and design a sideslip angle soft-sensor. In Section IV, the performance of the proposed soft-sensor is compared with CarSim. Finally, some conclusions are presented in Section V. The symbols are list in the appendix.

II. Vehicle Model

A. Lateral Dynamics Model

The non-linear two-track yaw plane vehicle is shown in Fig. 1.

P. Miao, G. Liu, D. Zhang,Y. Jiang, H. Zhang and H. Zhou are with the School of Electrical and Information Engineering, Jiangsu University, Zhenjiang 212013, China. G. Liu, (corresponding author; Tel: +86-0511-88791960; e-mail: ghliu@ujs.edu.cn).

This work was supported by the National Natural Science Foundation of China (61273154), the Specialized Research Fund for the Doctoral Program of Higher Education of China (Project 20123227110012), the innovation plan for PhD candidate of Jiangsu University (CX10B_014X), and the Priority Academic Program Development of Jiangsu Higher Education Institutions.

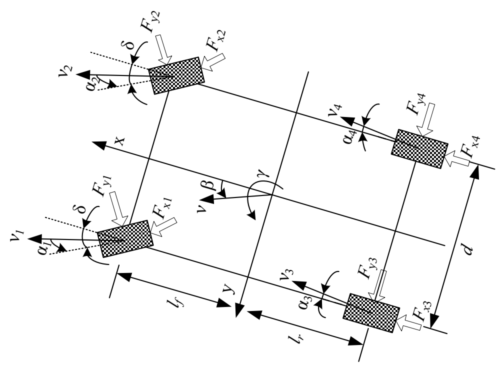

Fig. 1. Non-linear two-track yaw plane vehicle model.

The vehicle speed obtains from $v = (v_x^2 + v_y^2)^{1/2}$ with the body sideslip angle $\beta = \arctan(v_x / v_y)$. appears per page. The vehicle is assumed to have a low vehicle centre of gravity (CG) height with stiff suspension, and also the suspension dynamics and roll dynamics have no affect on the vehicle plane dynamics.

The equations for the vehicle speed, the sideslip angle and the yaw rate dynamics are displayed in the follows:

$$\begin{cases} \dot{v} = \dfrac{1}{m}((F_{x1}+F_{x2})\cos(\beta-\delta)+(F_{x3}+F_{x4})\cos\beta \\ \quad +(F_{y1}+F_{y2})\sin(\beta-\delta)+(F_{y3}+F_{y4})\sin\beta) \\ \dot{\beta} = \dfrac{1}{mv}(-(F_{x1}+F_{x2})\sin(\beta-\delta)-(F_{x3}+F_{x4})\sin\beta \\ \quad +(F_{y1}+F_{y2})\cos(\delta-\beta)+(F_{y3}+F_{y4})\cos\beta)-\gamma \\ \dot{\gamma} = \dfrac{1}{J_z}(F_{x1}(l_f\sin\delta-\dfrac{d}{2}\cos\delta)+F_{x2}(l_f\sin\delta+\dfrac{d}{2}\cos\delta) \\ \quad +\dfrac{d}{2}(F_{x4}-F_{x3})+F_{y1}(\dfrac{d}{2}\sin\delta+l_f\cos\delta) \\ \quad F_{y2}(-\dfrac{d}{2}\sin\delta+l_f\cos\delta)-l_r(F_{y3}+F_{y4})) \end{cases} \tag{1}$$

The coordinate frame of the equations is based on the CG as its origin fixed and with the center line of vehicle as the *x*-axis.

B. Tire Force and Tire Slip Angle

To better understand the motion of vehicles, we must study the tire force. The longitudinal force of the vehicle is generated by the in-wheel motor and the wheel rotational motion is shown in Fig. 2.

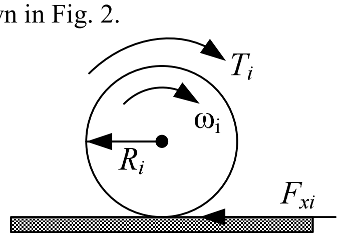

Fig. 2. Wheel rotational motion.

The longitudinal force is shown in the following equation:

$$F_{xi} = \frac{1}{R_i}(T_i - J_i \cdot \dot{\omega}_i) \tag{2}$$

With the assumption that the tire as a rigid body. So the rolling radius and rotational inertia are considered to be constant.

As this study is mainly focused on the estimation of the sideslip angle in non-linear region, the Dugoff's model is used as the tire model. The simplified non-linear lateral tire forces are shown in the follow:

$$F_{yi} = -C_i \tan\alpha_i f(\lambda) \tag{3}$$

Where C_i is the lateral stiffness, α_i is the slip angle, and $f(\lambda)$ is shown as:

$$f(\lambda) = \begin{cases} (2-\lambda)\lambda & if \quad \lambda < 1 \\ 1 & if \quad \lambda \geq 1 \end{cases} \tag{4}$$

$$\lambda = \frac{\mu F_{zi}}{2C_i|\tan\alpha_i|} \tag{5}$$

μ is the road coefficient and F_{zi} is the normal load on the tires. In order to simplify the model we assume the conditions is pure slip.

The normal load of the tire has three parts due to the effect of the lateral acceleration, the longitudinal acceleration and the roll of the vehicle. Without considering the roll of the vehicle, so the bank of angle is defined as $\Phi = 0$. The normal load of each tire can be described as:

$$\begin{cases} F_{z1} = \dfrac{mgl_r}{2(l_f+l_r)} - \dfrac{ma_xh}{2(l_f+l_r)} - \dfrac{K_{f\Phi}}{K_{f\Phi}+K_{r\Phi}} \cdot \dfrac{ma_yh}{d} \\ F_{z2} = \dfrac{mgl_r}{2(l_f+l_r)} - \dfrac{ma_xh}{2(l_f+l_r)} + \dfrac{K_{f\Phi}}{K_{f\Phi}+K_{r\Phi}} \cdot \dfrac{ma_yh}{d} \\ F_{z3} = \dfrac{mgl_f}{2(l_f+l_r)} + \dfrac{ma_xh}{2(l_f+l_r)} - \dfrac{K_{r\Phi}}{K_{f\Phi}+K_{r\Phi}} \cdot \dfrac{ma_yh}{d} \\ F_{z4} = \dfrac{mgl_f}{2(l_f+l_r)} + \dfrac{ma_xh}{2(l_f+l_r)} + \dfrac{K_{r\Phi}}{K_{f\Phi}+K_{r\Phi}} \cdot \dfrac{ma_yh}{d} \end{cases} \tag{6}$$

The tire slip angle α_i is shown as follow:

$$\begin{cases} \alpha_1 = \delta - arctan(\dfrac{v\beta + l_f\gamma}{v - \gamma d/2}) \\ \alpha_2 = \delta - arctan(\dfrac{v\beta + l_f\gamma}{v + \gamma d/2}) \\ \alpha_3 = -arctan(\dfrac{v\beta - l_r\gamma}{v - \gamma d/2}) \\ \alpha_4 = -arctan(\dfrac{v\beta - l_r\gamma}{v + \gamma d/2}) \end{cases} \tag{7}$$

III. NNLI Sideslip Angle Soft-Sensor

This section will illustrate the assumed inherent sensor and the NNLI sideslip angle soft-sensor [18-20].

A. Left Inverse Soft-Sensor Theory

A linear or non-linear system Σ with *q*-dimensional input $u(t) = (u_1, u_2, \cdots, u_q)^T$ and *d*-dimensional output $y(t) = (y_1, y_2, \cdots, y_d)^T$ can be represented by the state function:

$$\begin{cases} \dot{x} = f(x,u) \\ y = h(x,u) \end{cases}, \qquad x(t_0) = x_0 \tag{8}$$

The system statement is $x = (x_1, x_2, \cdots, x_n)^T \in R^n$ and given a certain initial state $x(t_0) = x_0$.

For a general point of view, the mathematical model of this system is equivalent to a mapping from the input to the output. It can be described as the following:

$$y(\cdot) = \theta(x_0, u(\cdot)) = \theta u \tag{9}$$

Generally speaking, for a non-linear system, in its interior, it can be assumed that there exists an assumed inherent sensor subsystem as shown in Fig. 3. The variables to be estimated are the inputs of the subsystem while the variables which can be measured directly are the outputs. The variables are the input variables of the controlled system. If a left inversion of the assumed inherent sensor can be constructed and cascaded behind the assumed inherent sensor, then a so-called composite identity system whose outputs would be the identity mapping of its inputs is obtained. It means that the outputs of the assumed inherent sensor inversion will reproduce completely the inputs of the "assumed inherent sensor". Therefore, the non-directly measured variables of the controlled system can be estimated from the variables which can be measured directly [17], [20].

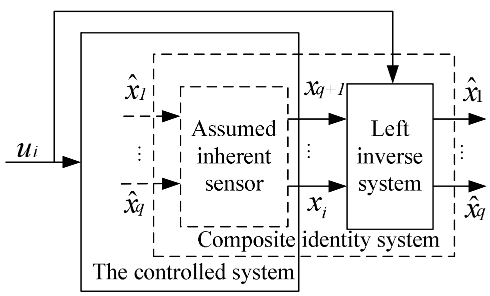

Fig. 3. The measuring principle based on left inversion.

B. NNLI Sideslip Angle Soft-Sensor

The static NN has the ability to approach the non-linear system. A NNLI sideslip angle soft-sensor based on the ability can be achieved. The basic idea of the NNLI sideslip angle estimator is as follows:

1) Construct an assumed inherent sensor.
2) Get the inversion of the assumed inherent sensor.
3) Using a static NN to approximate this inversion system.
4) Put the inversion system behind the assumed inherent sensor in series to produce a unified system, therefore, it is named as the NNLI.
5) Through this NNLI, we can realize the estimation of the non-directly measured sideslip angle.

For the system in (1), its state variable is

$$\boldsymbol{x} = (x_1, x_2, x_3, x_4)^T = (\gamma, \beta, v_x, a_x)^T \tag{10}$$

The input of the system is

$$u = [u_1, u_2, u_3]^T = [\delta, T_{d3}, T_{d4}]^T \tag{11}$$

The directly measured variable is

$$\begin{aligned} Z &= [z_1, z_2, z_3, z_4, z_5, z_6, z_7, z_8, z_9, z_{10}]^T \\ &= [v, \gamma, F_{x1}, F_{x2}, F_{x3}, F_{x4}, F_{y1}, F_{y2}, F_{y3}, F_{y4}]^T \end{aligned} \tag{12}$$

The non-directly measured variable is

$$x = [x_1]^T = [\beta]^T \tag{13}$$

According to the modeling algorithm, the Jacobian matrix rank is obtained.

$$rank\left(\frac{\partial Z^T}{\partial x}\right) = rank\left(\frac{\partial Z^T}{\partial \beta}\right) = rank\begin{pmatrix} 0 \\ 0 \end{pmatrix} = 0 \tag{14}$$

Since the rank is not equal to the number of the non-directly measured variables, it can be further derivate.

$$rank\left(\frac{\partial\left(z^T, \dot{z}^T\right)}{\partial x}\right) = rank\begin{pmatrix} 0 & 0 & 0 & 0 & 0 & 0 \\ \frac{\partial \dot{v}}{\partial \beta} & \frac{\partial \dot{\gamma}}{\partial \beta} & 0 & 0 & 0 & 0 \end{pmatrix} \tag{15}$$

As is shown in the following equation referred to (1):

$$\begin{aligned} \frac{\partial \dot{v}}{\partial \beta} &= -\frac{1}{m}((F_{x3} + F_{x4})\sin\beta + (F_{y1} + F_{y2})\cos(\beta - \delta) \\ &\quad + (F_{y3} + F_{y4})\cos\beta) \neq 0 \\ \frac{\partial \dot{\gamma}}{\partial \beta} &= \frac{1}{J_z} F_{y1}\left(\frac{d}{2}\cos\delta - l_f \sin\delta\right) \neq 0 \end{aligned} \tag{16}$$

The rank is as following:

$$rank\left(\frac{\partial\left(z^T, \dot{z}^T\right)}{\partial x}\right) = 1 \tag{17}$$

Therefore, the model of the assumed inherent sensor is left invertible. The left inversion model of the sideslip angle according to these functions can be achieved. And the inversion of the assumed inherent sensor for the sideslip angle can be written as:

$$\beta = \phi(v, a_x, a_y, T_{d1}, T_{d2}, T_{d3}, T_{d4}, \delta) \tag{18}$$

Since the vehicle is driven by two-rear-wheel, therefore

$$T_{d1} = T_{d2} = 0 \tag{19}$$

And the inversion of the assumed inherent sensor can be written as:

$$\beta = \phi(v, a_x, a_y, T_{d3}, T_{d4}, \delta) \tag{20}$$

As the system is complex in mathematical model, it is difficult to construct the inversion of the assumed inherent sensor by analytic means. Hence, a static NN is used to approximate the above nonlinear function in (20). Then, the NNLI dynamic soft-sensing model is finally completed, which is composed of a static NN and a series of differentiators. This simplifies the construction of the proposed NN-based soft-sensor in practical use, while it is strict enough in theory. The structure of the NNLI sideslip angle soft-sensor is shown in Fig. 4.

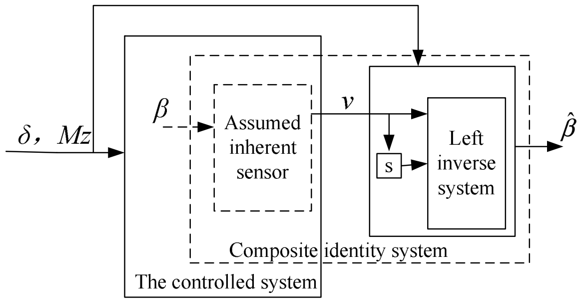

Fig . 4. NNLI sideslip angle estimator.

IV. Simulation Result

The performance of the proposed soft-sensor is evaluated by Matlab/Simulink-CarSim co-simulation. A vehicle with two in-motors at the rear wheels is developed using CarSim. The NNLI soft-sensor is constructed by using Matlab/Simulink.

A. NNLI Train

A NN should be trained and tested by means of numerical data in the first step. In order to highlight the performance of the NNLI sideslip angle soft-sensor in non-linear condition, the range of vehicle speed is chosen comparatively high one.

At the same time, the variable steering wheel angle is necessary for inspiring the NN sufficiently. The set of maneuvers for NN training is shown in Figs. 5 and 6.

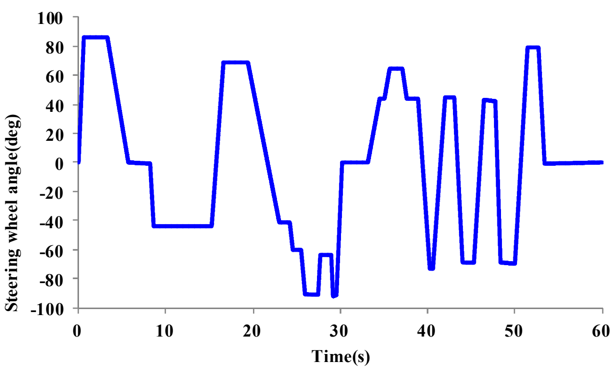

Fig. 5. Signal of steering wheel angle for training.

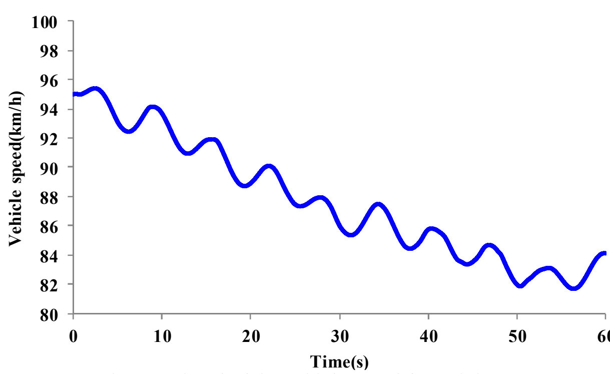

Fig . 6. Signal of the vehicle speed for training.

Meanwhile, a static back propagation NN with the structure of 11-18-1 with "tan sigmoid" transfer function on the nodes of one hidden layer, and "linear" transfer function on the node of output layer is adopted. The training mean squared error is 9.999e-4 after 515 times of training by using Levenberg-Marquardt algorithm. In addition, to improve the training performance and enhance the soft-sensing performance, all the data are normalized within [-1, 1].

B. NNLI Sideslip Angle Result

Two Simulations are carried out under a single lane change maneuver and a step maneuver. In two maneuver simulations, the vehicle travels on a wet road (μ=0.4) at a constant speed of 90 km/h. The estimated sideslip angle is compared with the output of CarSim in order to reflect the superiority of NNLI soft-sensor.

As shown in Figs. 7 and 8, simulation results verify that the actual (denoted as CarSim) and estimated values (denoted as NNLI) of the sideslip angle agree well. Therefore, the NNLI soft-sensor can accurately predict the sideslip angle. The presented algorithm is proved perfect in theory verification and the simulation.

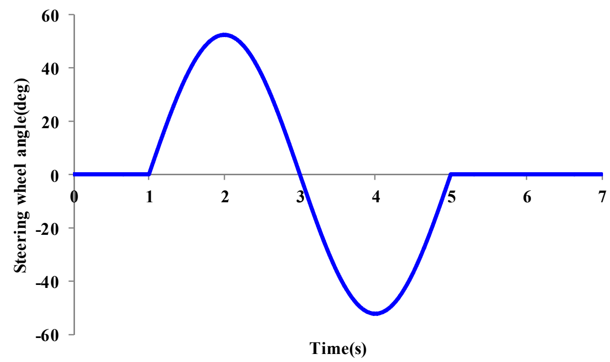

(a) Single sine steering angle.

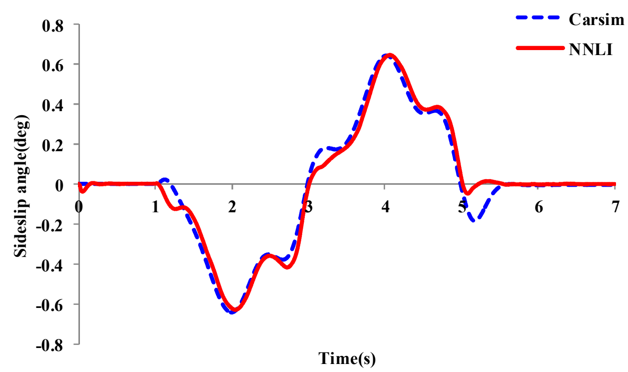

(b) Comparison of actual and estimated values of sideslip angle.

Fig . 7. Simulation under single lane change maneuver.

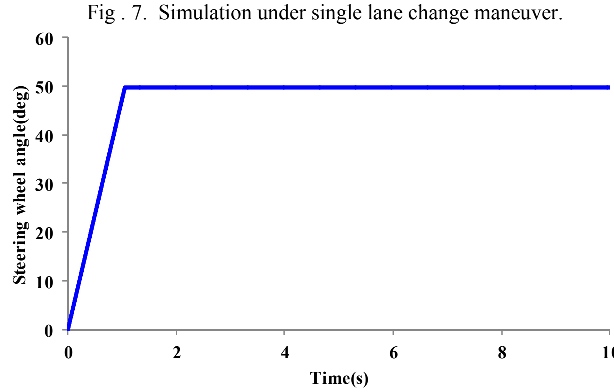

(a) Front steering angle.

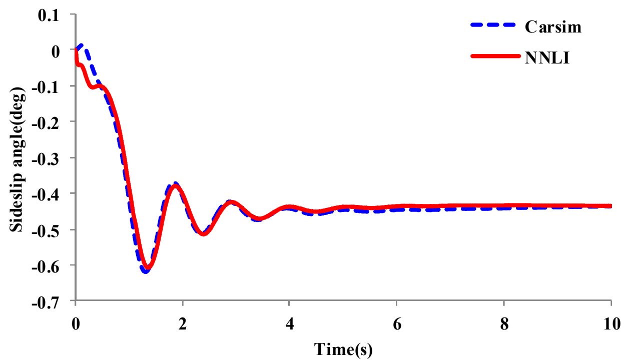

(b) Comparison of actual and estimated values of sideslip angle.
Fig . 8. Simulation under step maneuver

V. CONCLUSION

The system of the vehicle is non-linear and the common observe methods can hardly track the state of the vehicle. But the soft-sensor based on NNLI is perfect in estimating the non-linear state of the vehicle. In this paper, to estimate the sideslip angle, a new method for sideslip angle estimation has been presented. The NNLI has been treated as the dynamic soft-sensor, which consists of a NN and a series of differentiators. And its performance has been investigated through CarSim-Matlab/Simulink co-simulation. The vehicle with the proposed NNLI soft-sensor can successfully follow the sideslip angle trajectory.

APPENDIX

TABLE I
NOMENCLATURE

Symbol	MEANING
a_x	Longitudinal acceleration at CG (center of gravity)
a_y	Lateral acceleration at CG
v_x	Longitudinal speed at CG
v_y	Lateral speed at CG
d	Track width
g	Acceleration due to gravity
l_f	Distance from CG to front axle
l_r	Distance from CG to rear axle
i	1,2,3 and 4 corresponding to front left, front right, Rear left and rear right
m	Total mass of vehicle
C_i	Tire cornering stiffness at the ith tire
R_i	Rolling radius at the ith tire
F_{xi}	Longitudinal tire force at the ith tire
F_{xi}	Lateral tire force at the ith tire
v	Vehicle speed at CG
J_z	Vehicle inertia around the z-axis
J_i	Wheel angular moment of inertia at the ith tire
T_i	In-wheel motor torque applied to the ith tire
v_i	Wheel speed at the ith tire
ω_i	Wheel angular velocity at the ith tire.
β	Vehicle sideslip angle
δ	Front steering angle
γ	Yaw rate
$K_{f\Phi}$	Roll stiffness coefficient of front axle
$K_{r\Phi}$	Roll stiffness coefficient of rear axle

REFERENCES

[1] Y. Hori, "Future vehicle driven by electricity and control-research on four wheel-motored 'UOT Electric March II'," *IEEE Trans. Ind. Electron.,* vol. 51, no. 5, pp. 954-962, Oct. 2004.

[2] K. Nam, S. Oh and H.Fujimoto, "Estimation of sideslip and roll angles of electric vehicles using lateral tire force sensors through RLS and Kalman filter approaches," *IEEE Trans. Ind. Electron*., vol. 60, no. 3, pp. 988-1000, Jan. 2013.

[3] D. Yin, S. Oh, and Y. Hori, "A novel traction control for EV based on maximum transmissible torque estimation," *IEEE Trans. Ind. Electron*., vol. 56, no. 6, pp. 2086-2094, Jun. 2009.

[4] F. Chelli, E. Sabbioni, M. Pesce, and S. Melzi, "A methodology for vehicle sideslip angle identification: Comparison with experimental data," *Veh. Syst. Dyn.,* vol. 45, no. 6, pp. 549-563, Jun. 2007.

[5] M. C. Best, T. J. Gordon, and P. J. Dixon, "An extended adaptive kalman filter for real-time state estimation of vehicle handling dynamics," *Veh. Syst. Dyn.,* vol. 34, no. 1, pp. 57-75, Jul. 2000.

[6] G. Cong, L. Mostefai, M. Denai, and Y. Hori, "Direct yaw-moment control of an in-wheel-motored electric vehicle based on body slip angle fuzzy observer," *IEEE Trans. Ind. Electron*., vol. 56, no. 5, pp. 1411-1419, May. 2009.

[7] M. Doumiati, A. C. Victorino, A. Charara, and D. Lechner, "On board real-time estimation of vehicle lateral tire-road forces and sideslip angle," *IEEE ASME. Trans. Mechatron.*, vol. 16, no. 4, pp. 601-614, Aug. 2011.

[8] X. Gao, Z. Yu, J. Neubeck, and J. Wiedemann, "Sideslip angle estimation based on input-output linearization with tire-road friction adaptation," *Veh. Syst. Dyn.,* vol. 48, no. 2, pp. 217-234, Feb. 2010.

[9] S. You, J. Hahn, and H. Lee, "New adaptive approaches to real-time estimation of vehicle sideslip angle," *Control Eng. Pract*., vol. 17, no. 12, pp. 1367-1379, Dec. 2009.

[10] D. Piyabongkarn, R. Rajamani, J. Grogg, and J. Lew, "Development and experimental evaluation of a slip angle estimator for vehicle stability control," *IEEE Trans. Control Syst. Technol.,* vol. 17, no. 1, pp. 78-88, Jan. 2009.

[11] D. M. Bevly, J. Ryu, and J. C. Gerdes, "Integrating INS sensors with GPS measurements for continuous estimation of vehicle sideslip, roll, and tire cornering stiffness," *IEEE Trans. Intell. Transp. Syst*., vol. 7, no. 4, pp. 483-493, Dec. 2006.

[12] D. M. Bevly, J. C. Gerdes, and C. Wilson, "The use of GPS based velocity measurements for measurement of sideslip and wheel slip," *Veh. Syst. Dyn.*, vol. 38, no. 2, pp. 127-147, Feb. 2003.

[13] F. Cheli, S. Melzi, M. Pesce, and E. Sabbioni, "A methodology for vehicle sideslip angle identification: comparison with experimental data," *Veh. Syst. Dyn.*, pp. 549-563, Jun. 2007.

[14] S. Melzi and E. Sabbioni, "On the vehicle sideslip angle estimation through neural networks: numerical and experimental results," *Mech. Syst. Signal Process*, vol. 25, no. 6, pp. 2005-2019, Aug. 2011.

[15] S. Solmaz, "Simultaneous estimation of road friction and sideslip angle based on switched multiple non-linear observers," *IET. Control Theory Appl.*, vol. 6, no. 14, pp. 2235-2247, Sep. 2012.

[16] K. Nam, H. Fujimoto and Y. Hori, "Lateral stability control of in-wheel-motor-driven electric vehicles based on sideslip angle estimation using lateral tire force sensors," *IEEE Trans. Veh. Technol*, vol. 61, no. 5, pp. 1972-1985, 2012.

[17] Dai X., Wang W., and Ding Y., "'Assumed inherent sensor' inversion based ANN dynamic soft-sensing method and its application in erythromycin fermentation process," *Comput. Chem. Eng*., vol. 30, no. 8, pp. 1203-1225, Jun. 2006.

[18] Dai X. , and Ding Y. , "ANN inversion based soft-sensing of biochemical parameters in erythromycin fermentation," *Proc. Int. Conf. Inf. Acquis*., pp. 262-266, Jun. 2004.

[19] Ding Y. , Dai X. , and Wang W. , "Modified Soft-sensing Method of Erythromycin Fermentation Process Variables Based on "assumed inherent sensor" inversion," *Proc. Int. Conf. Inf. Acquis., ICIA,* pp. 201-205, Jul. 2007.

[20] Ding Y, Liu G, Dai X. "Soft-sensing method based on modified ANN inversion and its application in erythromycin fermentation," *IEEE Int. Conf. Inf. Autom., ICIA,* pp. 900-905, Jun. 2012.